

# Laser Forward Transfer of Functional Materials for Digital Fabrication of Microelectronics

Alberto Piqué, Heungsoo Kim, and Raymond C.Y. Auyeung

Materials Science and Technology Division, Code 6364, Naval Research Laboratory, Washington, DC 20375

E-mail: pique@nrl.navy.mil

Andrew T. Smith

Nova Research Inc., Alexandria, VA 22308

**Abstract.** Laser-induced forward transfer, or LIFT, is a direct-write technique that enables nozzle-free, non-contact printing of 3-dimensional pixels or voxels of suspensions of functional materials across a wide range of viscosities with micrometer resolution. Printing of low-viscosity (<0.1 Pa s) nanoparticle (NP) inks by LIFT is in many ways similar to inkjet printing, where the cured voxel size and shape are determined by its interaction with the substrate. LIFT is also compatible with NP pastes of very high viscosity (>100 Pa s) and high solids content (>80 wt%), resulting in printed voxels that precisely replicate the shape and size of the laser transferring pulse. This LIFT regime, known as laser decal transfer or LDT, allows the congruent printing of highly loaded colloids and suspensions, unlike any existing direct-write process. This work compares LIFT of low-viscosity NP inks with LDT of high-viscosity NP pastes in terms of the voxels of silver NP suspensions printed by each technique. It also presents advances in a new digital fabrication technique using a spatial light modulator to change the size and shape of the LDT laser pulse, resulting in the dynamic reconfiguration of individual voxels. This enables a new level of parallelization unlike current serial direct-write processes, since each voxel can be varied according to the pattern design. An overview of the opportunities and challenges associated with LIFT of NP suspensions forms part of the conclusions. ©2013 Society for Imaging Science and Technology.

[DOI: 10.2352/J.ImagingSci.Technol.2013.57.4.040404]

## INTRODUCTION

Direct-write processes are evolving into viable techniques for printing functional materials over diverse types of surfaces for the digital fabrication of microelectronic devices. These simple, relatively fast, low cost and environmentally friendly alternatives to traditional photolithographic processes have the potential to completely change the way microelectronics are presently fabricated. Given the digital nature of direct-write processes, i.e., no need for masks or etching of excess material, their integration into existing production lines would enable their use where fast prototyping or batch customization is required. Overall, data driven patterning techniques such as direct-write processes represent a competitive alternative to optical lithography systems for the microfabrication of electronic, optical, sensor and power generating structures.<sup>1</sup>

A description of the numerous types of direct-write techniques currently available is beyond the scope of this work and the reader is referred to the review articles by Hon et al.<sup>2</sup> and Zhang et al.,<sup>3</sup> and the book edited by Piqué and Chrisey.<sup>1</sup> In general, direct-write processes rely on the dispensing, transfer or printing of discrete lumps of material known as voxels (i.e., volumetric 3D pixels) at predetermined locations on a substrate. These voxels serve as the building blocks for the lines, sheets and 3D structures required to fabricate a device. Among these voxel-depositing direct-write processes, inkjet printing is one of the most widely used techniques to date given its ability of non-contact printing of a wide range of functional fluids and inks.<sup>4</sup> However, in order to avoid clogging and/or corrosion of the dispensing nozzles, inkjet printing is limited to the transfer of low-viscosity, chemically benign nanoparticle suspensions. In addition, the printing of patterns with well defined edge features by inkjet is very difficult given the variable behavior of fluids on different surfaces and their resulting instability due to wetting effects.<sup>5,6</sup>

Laser-induced forward transfer, or LIFT, is a non-contact, nozzle-free additive process in which a controlled amount of complex material is transferred from a donor film (or ribbon) to a receiving substrate upon interaction with a laser pulse,<sup>7</sup> as shown schematically in Figure 1. Due to its nozzle-free nature, LIFT is capable of printing voxels of nanoink suspensions with wider ranges of viscosity than inkjet, thus significantly reducing variations due to wetting and drying effects.<sup>8</sup> When LIFT is applied to high-viscosity pastes, it is possible for the printed voxel to match congruently the illuminating laser pulse, as shown in Fig. 1(b). This process, referred to as laser decal transfer or LDT,<sup>9</sup> offers a unique approach to direct-writing techniques in which voxel shape and size become controllable parameters, allowing the non-lithographic generation of thin-film-like structures for a wide range of applications such as circuit repair,<sup>10</sup> metamaterials,<sup>11</sup> 3D interconnects,<sup>12</sup> freestanding structures<sup>13,14</sup> and membranes.<sup>15</sup> The ability to modify the voxel shape and size according to the desired final pattern allows an increase in the resolution and speed of the printing process. Single voxels with the desired shape can be used to directly form complex structures in one single transfer step, reducing the processing time as well as avoiding

Received May 3, 2013; accepted for publication Aug. 15, 2013; published online Jul. 1, 2013. Guest Editors: Jolke Perelaer and Jim Stasiak.

1062-3701/2013/57(4)/040404/8/\$20.00

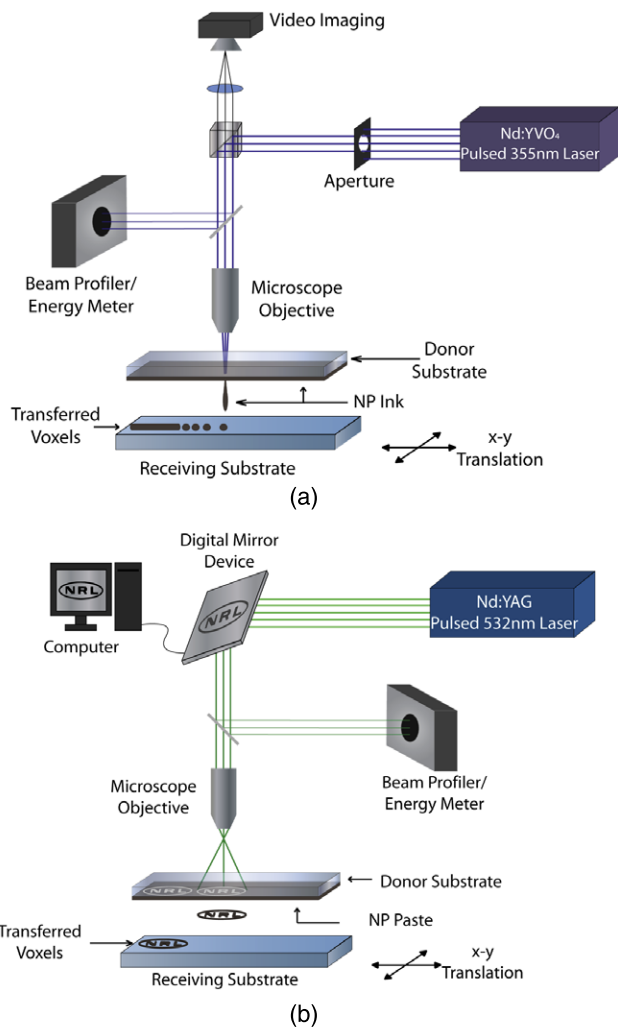


**Figure 1.** Schematic diagrams illustrating the basic elements of a laser-induced forward transfer (LIFT) system. Configuration with the laser profile shaped by (a) an aperture and (b) a digital micromirror device (DMD). The aperture is used with LIFT of low-viscosity NP inks and high-viscosity NP pastes, while the DMD is used with laser decal transfer (LDT) of high-viscosity NP pastes only.

problems related to the merging of multiple voxels, which are prevalent with inkjet.<sup>16</sup> Thus, printing shaped voxels increases the capabilities of LIFT as well as its potential degree of parallelization, as shown by dynamically adjusting the spatial profile of individual laser pulses.<sup>17,18</sup>

In this work, we present a side-by-side comparison of LIFT of low-viscosity ( $<0.1$  Pa s) silver nanoparticle (NP) inks with LDT of high-viscosity ( $>100$  Pa s) silver NP pastes. Examples of voxels that were laser transferred under similar conditions (laser spot size, shape and pulse energy) for each NP suspension are shown together with examples of line and grid patterns generated with the two laser transfer techniques. We then show results obtained by performing LDT using a spatial light modulator. The spatial light modulator, based on a commercial digital micromirror device or DMD, allows dynamic adjustment of the size and shape of the laser pulse and thus the ability to print reconfigurable congruent voxels. The impact of

this capability, not available with current digital fabrication techniques, will be discussed. Overall, this article highlights the opportunities and current challenges encountered with LIFT of low-viscosity fluids and LDT of high-viscosity pastes for the digital fabrication of 2D and 3D structures of functional materials.

## EXPERIMENTAL METHODS

The experimental details of LIFT using an aperture<sup>19</sup> or a DMD<sup>20</sup> have been described elsewhere. Low-viscosity silver NP inks (CCI-300, nominal viscosity 0.01 Pa s, 20 wt% solids loading, Cabot Corp.) and high-viscosity silver NP pastes (NPS, nominal viscosity  $\sim 100$  Pa s, 80 wt% solids loading, Harima Chemicals Inc.) were the source materials for laser transfers. Donor substrates were prepared by either spin-coating the low-viscosity ink onto fused silica disks or doctor blading the high-viscosity paste into wells previously etched into transparent substrates (borosilicate glass). The actual thickness of the spin-coated ink layer or paste layer in the wells was nominally 1–2  $\mu\text{m}$ , as determined by confocal microscopy. Once transferred, the Ag patterns were oven cured at 100–150°C (for scanning electron microscope or SEM imaging) for 30 min or 180°C (for electrical characterization) for 1 h.

Laser transfers of both low- and high-viscosity inks/pastes onto receiving substrates were performed using a Spectra-Physics YHP40-355Q, frequency tripled Nd:YVO<sub>4</sub> laser ( $\lambda = 355$  nm) with a pulse width of approximately 30 ns and a Gaussian spatial beam profile. Laser decal transfer experiments with a DMD (Texas Instruments DLP-D4100 0.7" UV XGA kit) employed a Big Sky Laser/Quantel ULTRA CFR, frequency doubled, Nd:YAG laser ( $\lambda = 532$  nm) with a pulse width of approximately 10 ns and a multimode beam profile.

For the 355 nm laser, an aperture was used to remove the lower intensity periphery of the Gaussian beam which resulted in a more uniform spatial beam profile. This aperture was imaged through a 10 $\times$  microscope objective (OFR LMU-10 $\times$ -351) and defined the size and shape of the illuminated area on the donor substrate. Circular (and square) apertures of nominally 200, 275 and 390  $\mu\text{m}$  diameter (side-length) were used to generate imaged circular (square) spots of 22, 30 and 44  $\mu\text{m}$  diameter (side-length) respectively. Various sized rectangular apertures were used for laser transfers of continuous lines and freestanding structures using high-viscosity paste.

With the 532 nm laser, the multimode beam profile provided more uniform illumination of the DMD array, so an aperture was not required. The DMD was placed in the optical path of the laser beam before the focusing optics, replacing the metal aperture, as shown in Fig. 1(b). The reflected beam was then directed to the donor substrate and imaged through a 10 $\times$  microscope objective (OFR LMU-10 $\times$ -NUV) or a 5 cm f.l. lens (for larger area transfers) onto the receiving substrate. Control of the pattern in the DMD and picking of the laser pulse were

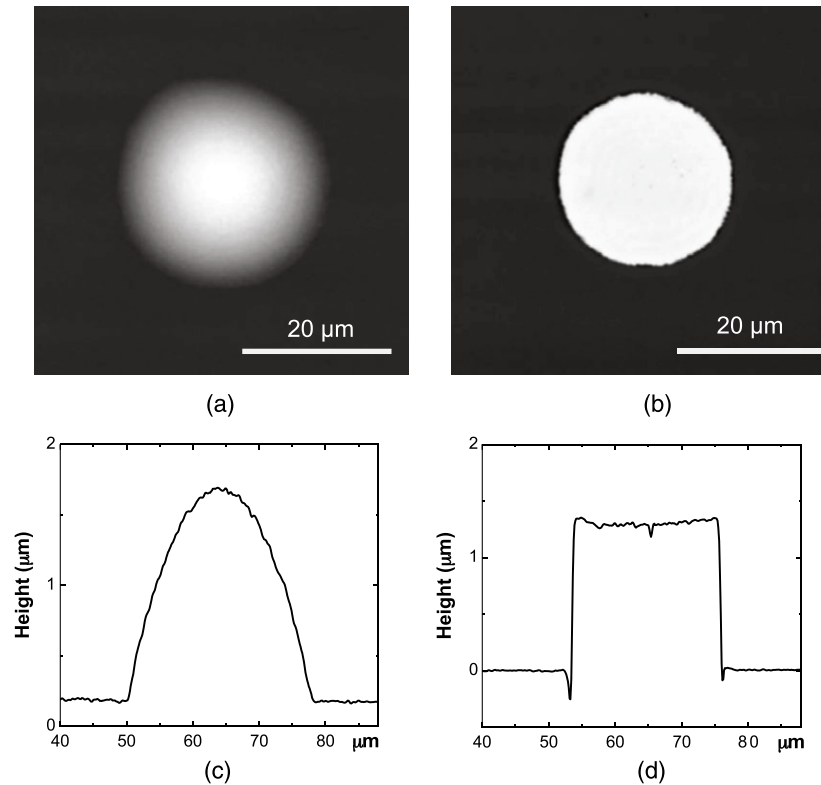


**Figure 2.** Confocal microscope images of voxels as-printed using a 22  $\mu\text{m}$  circular laser spot by (a) LIFT of low-viscosity Ag NP ink and (b) LDT of high-viscosity Ag NP paste on Si substrates. Optical profilometry displaying the diameter of the uncured voxels for (c) low-viscosity Ag NP ink (28  $\mu\text{m}$ ), and (d) high-viscosity Ag NP paste (22  $\mu\text{m}$ ).

set up independently or controlled simultaneously by a computer-controlled motion control system.

The laser fluences used were just above the transfer threshold and ranged between 60 and 70  $\text{mJ}/\text{cm}^2$  after the circular or square aperture or after the DMD. A beam splitter placed after the aperture or DMD was used to direct a small fraction of the beam ( $\sim 4\%$ ) to an energy meter (Ophir-Spiricon PD10 or PE9) and a beam profiler (Coherent LaserCam or Spiricon FX-50) to monitor the pulse energy and its spatial profile, respectively. An acousto-optic modulator (AOM) controlled the 355 nm laser pulse energy and timing, while a pulse generator (Stanford Research Systems DG535) controlled the 532 nm pulse energy by varying the Q-switch delay to the laser.

Before curing, the transfers were characterized by optical microscopy (Olympus BX51) or confocal microscopy (Olympus LEXT OLS3000). After curing, the transfers were characterized by contact profilometry (KLA Tencor P-16), SEM (JEOL JSM-7001F) or atomic force microscopy (AFM) (Digital Instruments Dimension 3100). Electrical characterization of fully cured transfers was performed using four-point Kelvin probes (Cascade Microtech M150 probe station) connected to a computer-controlled current source (Keithley 2400 sourcemeter).

## RESULTS AND DISCUSSION

Laser direct-write of low-viscosity NP suspensions using LIFT allows the generation of arbitrary patterns over most

types of surfaces in similar fashion to inkjet. The laser transfer of NP suspensions of functional materials such as metals,<sup>20</sup> transparent conductors<sup>21</sup> and dielectrics<sup>22</sup> has been demonstrated previously. LIFT of low-viscosity ( $< 0.1 \text{ Pa s}$ ) NP inks results in the deposition of discrete spherical voxels, as shown by the confocal microscope image in Figure 2(a) and the optical profile in Fig. 2(c) for silver NP ink on a Si substrate. The transfer of the same voxels sufficiently close to each other causes them to coalesce into lines, which can then fuse into the desired pattern. As with inkjet, printing of precise patterns using LIFT of low-viscosity NP inks is difficult given the variable behavior of fluids on different types of surfaces and their resulting instability due to wetting effects.<sup>6</sup> In fact, just like with inkjet, the laser transferred low-viscosity NP voxel undergoes spreading upon impact onto the substrate, then wets the substrate, and finally solidifies or evaporates depending on the rate at which it changes phase from liquid to solid. Together, these three processes will influence the shape and morphology of the final solid deposit and determine the achievable feature size and resolution limits.<sup>5</sup>

Raising the viscosity of the printed voxels by increasing their solids loading minimizes the variability due to wetting effects and at the same time reduces shrinkage during curing, leading to better control of the size and shape of the final patterns. This strategy works well with filamentary-based dispensing techniques,<sup>23</sup> but it is not compatible with drop-on-demand-based techniques such as inkjet, due to

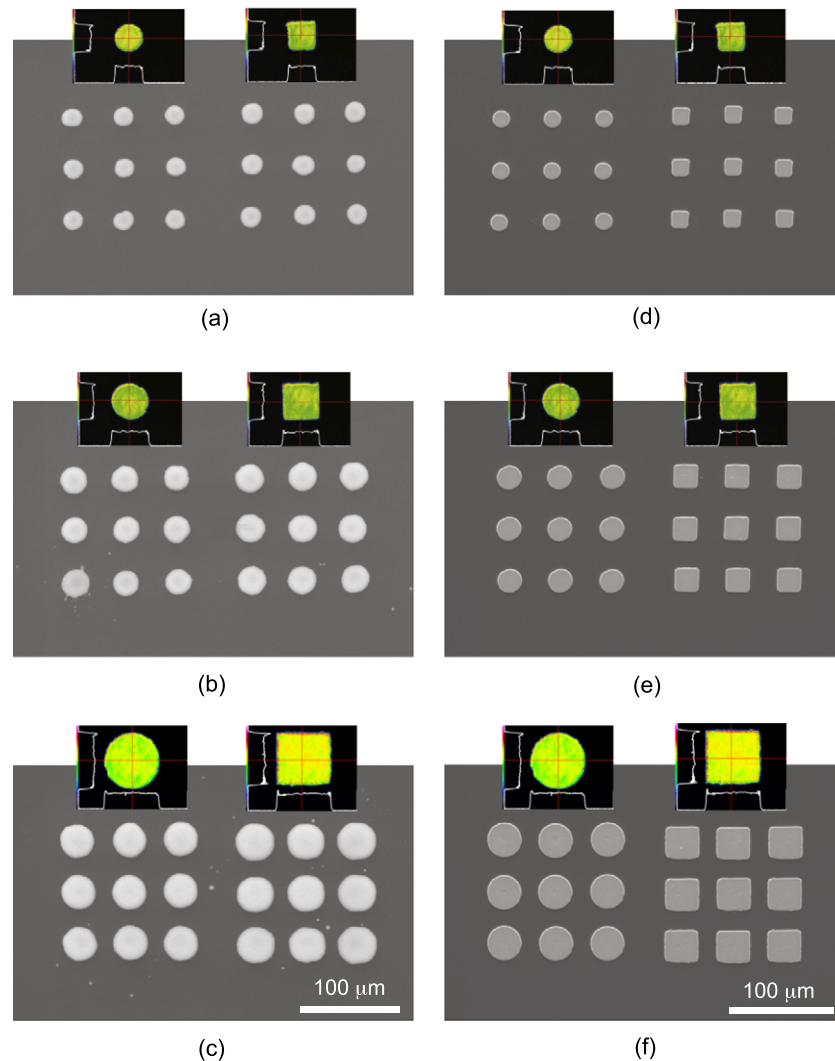


**Figure 3.** SEM images of arrays of voxels printed by (a)–(c) LIFT of low-viscosity Ag NP ink and (d)–(f) LDT of high-viscosity Ag NP paste on Si substrates. The images show three different sized arrays of circular- and square-shaped laser pulses: (a,d) 22, (b,e) 30 and (c,f) 44  $\mu\text{m}$ . The insets show the beam profile recorded for each beam. Only the LDT of high-viscosity Ag NP paste resembles the incident beam profile.

clogging of the nozzles. However, with laser direct-write this is not an issue, as demonstrated in Fig. 2(b) by the LDT of high-viscosity ( $>100 \text{ Pa}\cdot\text{s}$ ), high solids loading ( $\sim 80 \text{ wt}\%$ ) silver NP pastes. As the confocal microscopy image shows, the shape of the disk-shaped voxel of uncured NP paste is immune to spreading and wetting effects and retains its uniform cross section along the diameter of the transferring laser pulse (22  $\mu\text{m}$ ); see the profile scan in Fig. 2(d). This is not the case with LIFT of NP ink, where the low-viscosity fluid spreads and forms a spherical drop of uncured suspension, which will dry non-uniformly across a larger 28  $\mu\text{m}$  diameter disk.

Furthermore, with LDT of high-viscosity NP pastes both the shape (disks and squares) and the size (22, 30 and 44  $\mu\text{m}$  in diameter or length) of the incident laser pulses are reproduced by the voxels, as shown in the SEM images on the right side in Figure 3, which is not possible with LIFT of low-viscosity inks, as the cured transfers on the left side in Fig. 3 illustrate. For this test, voxels of silver NP ink and

silver NP paste were laser printed onto a Si substrate under the same conditions using six different laser spots (three circular and three square). The insets in each frame show the beam profiles for each laser spot displayed on the same scale. Note how the size of the voxels increases with increasing laser spot for both types of ink, but only the voxels obtained with LDT of silver NP paste form shapes congruent with the laser spots. This simple demonstration illustrates one of the great advantages of LDT for digital fabrication: the difference between the desired pattern and the actual voxel size and shape is minimal, thus guaranteeing that the printed structures will match the design.

Analysis of the resulting lines formed by overlapping voxels printed by LIFT of NP inks and LDT of NP pastes reveals what happens when multiple voxels coalesce. In the SEM image in Figure 4(a) the progressive decrease in voxel spacing ( $\Delta x = 70, 50, 30, 20$  and  $10 \mu\text{m}$ ) for LIFT of low-viscosity Ag NP inks eventually leads to their overlap into continuous lines. However, careful

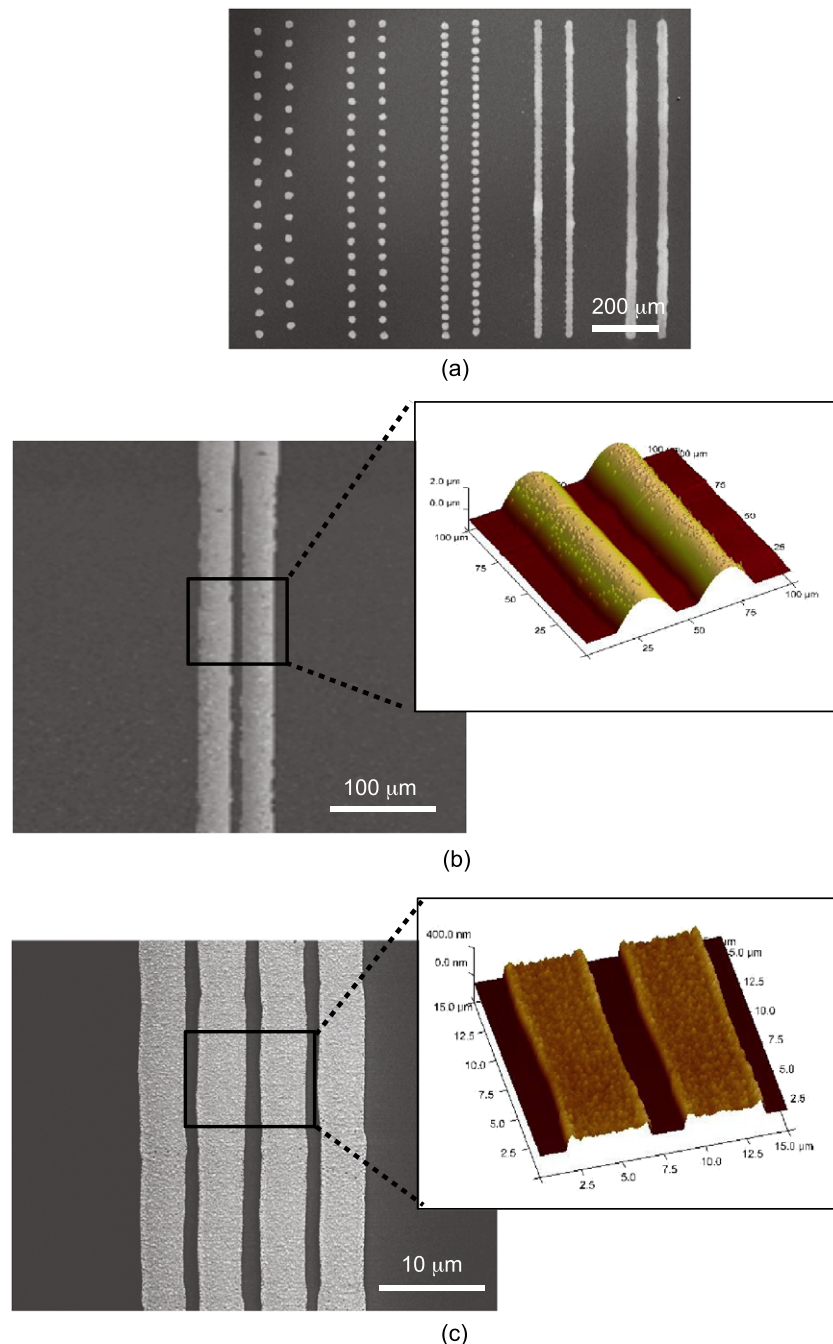


**Figure 4.** SEM images of printed lines on Si substrates by LIFT of low-viscosity Ag NP ink with (a) different voxel spacing ( $\Delta x = 70, 50, 30, 20$  and  $10 \mu\text{m}$  from left to right) and (b) fixed voxel spacing ( $\Delta x = 15 \mu\text{m}$ ). The inset in (b) shows an AFM 3D image ( $100 \mu\text{m} \times 100 \mu\text{m}$ ) of the lines. (c) SEM image of lines printed on a Si substrate by LDT of high-viscosity Ag NP paste, formed by stitching  $15 \mu\text{m}$  long by  $5 \mu\text{m}$  wide voxels, with  $\Delta x = 15 \mu\text{m}$  voxel spacing. The inset in (c) shows an AFM 3D image ( $15 \mu\text{m} \times 15 \mu\text{m}$ ) of the lines.

examination of these lines reveals scalloping for the first pair ( $\Delta x = 20 \mu\text{m}$ ) and some bulging for the second ( $\Delta x = 10 \mu\text{m}$ ), in agreement with a recent report for LIFT of a 50/50 by volume water/glycerol solution,<sup>24</sup> and this is similar to results obtained with inkjet printing of Ag NP inks.<sup>25</sup> It is possible, however, to obtain  $25 \mu\text{m}$  wide lines with  $10 \mu\text{m}$  gaps (corresponding to a  $35 \mu\text{m}$  pitch) with very good uniformity with LIFT of Ag NP inks for  $\Delta x = 15 \mu\text{m}$ , as the SEM image and AFM inset in Fig. 4(b) show. However, as these results reveal, it will be very difficult to reduce the

width of the lines or their pitch much further without them merging into one single patch. To achieve higher resolutions it is necessary to use instead LDT of high-viscosity Ag NP pastes, as demonstrated by the  $5 \mu\text{m}$  wide lines with  $2 \mu\text{m}$  gaps (corresponding to a  $7 \mu\text{m}$  pitch) in Fig. 4(c). It is important to note that despite the high viscosity of the silver NP paste required by the LDT process, the voxels are sufficiently fluid to fuse with their nearest neighbors after transfer, thus generating continuous patterns, as the lines in Fig. 4(c) demonstrate. Previous work has shown these LDT

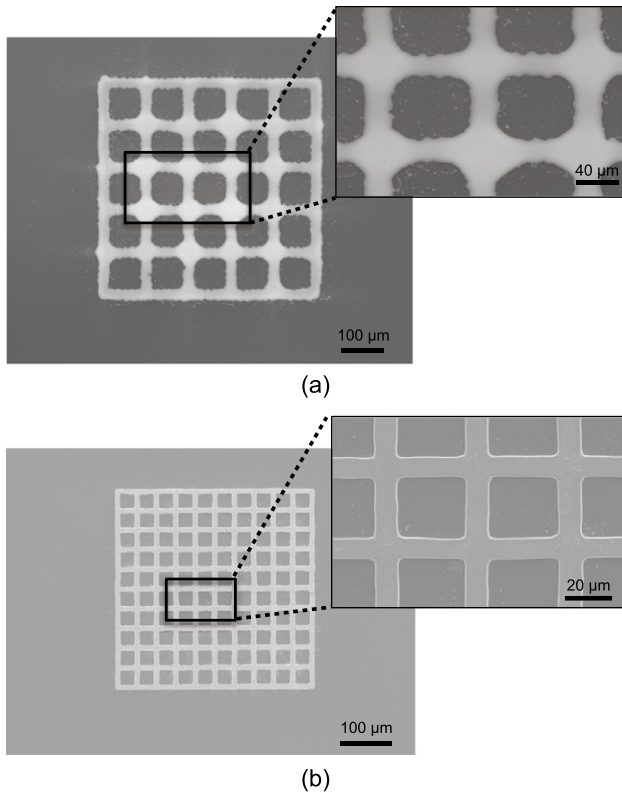


**Figure 5.** Printing of square grids on Si substrates by (a) multiple voxels of low-viscosity Ag NP ink and (b) a single laser pulse of high-viscosity Ag NP paste using a grid image generated by a DMD.

printed lines to exhibit resistivities of  $\sim 2\times$  those of bulk silver ( $3.4 \mu\Omega \text{ cm}$ ).<sup>10</sup>

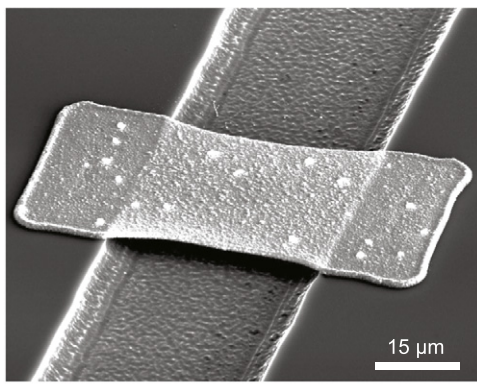
Another type of structure that illustrates the advantages of printing high-viscosity and heavy-particle-loading NP pastes is a simple grid. In a grid, the overlapping lines undergo bulging and loss of resolution due to printing of excess material over the intersections, as the SEM images of a grid printed by LIFT of low-viscosity Ag NP ink on a Si substrate in Figure 5(a) demonstrate. Better resolution can be achieved with LDT of high-viscosity Ag NP paste, but the line overlap at the intersections can still be a problem. Printing a design consisting of continuous lines in one direction and non-overlapping segments in the other direction would mitigate this; however, a better solution is to print the entire grid with one single laser pulse using LDT of Ag NP paste with a DMD, as shown in Fig. 5(b). The use of the DMD allows the shaping of the laser pulse in the form of the required grid and the congruent nature of the voxels generated by LDT guarantees that the shape and pattern of the laser pulse is not lost.

Compared with other LIFT processes, LDT takes place at very low laser energy densities (or fluences). As a result the voxels are released from the ribbon with very low kinetic energies, minimizing the stress and deformation of the voxels when they land on the receiving substrate. The high degree of control of size and shape achievable with LDT has been applied to the digital microfabrication of 3-dimensional stacked assemblies and freestanding struc-

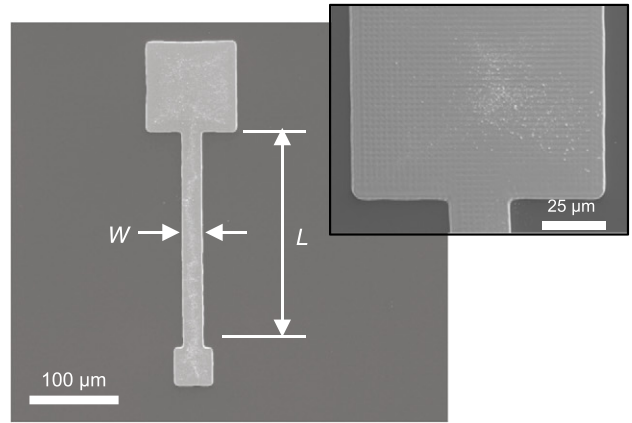
tures such as microbridges and microcantilevers without the use of sacrificial layers.<sup>13–15,26</sup> Figure 6(a) shows an example of one such freestanding microbridge formed over a trench in a Si substrate by LDT of Ag NP paste. This structure was formed in one single step by laser printing the voxel across the gap without the use of sacrificial support layers. In principle, as long as the energy distribution across the laser spot is uniform and above the transfer threshold, LDT can be used to print voxels of arbitrarily large area. This is shown in the pattern in Fig. 6(b), which extends over 1 mm in one direction with the NRL (Naval Research Lab) oval seal generated by the DMD image and printed with a single laser pulse. Note that a printed linewidth of  $<25 \mu\text{m}$  can be maintained over the  $1 \text{ mm}^2$  area. This pattern, which represents a change in printed area of over a factor of 2500 from those shown in Fig. 2(b), illustrates the capability of combining LDT of high-viscosity pastes with the DMD laser spatial control. In Fig. 6(c) an example of an actual application of these techniques is shown corresponding to a single voxel printed by LDT of Ag NP paste using a DMD. Arrays of these metamaterial inspired antennas can be printed readily in this way and their size and shape can be changed instantaneously without interrupting the process. This capability exemplifies some of the advantages of the laser direct-write processes described in this work when compared to other direct-write techniques.

An example of dynamically reconfigurable voxels made by LDT with a DMD-shaped laser pulse for interconnect applications is provided in Figure 7. The basic pattern comprised of two pads connected by a  $250 \mu\text{m}$  long,  $25 \mu\text{m}$  wide and  $0.8 \mu\text{m}$  thick line is shown in Fig. 7(a). In this particular case, three distinct interconnect designs were used, which were loaded into the DMD and LDT printed next to each other, as seen in Fig. 7(b). The printing of each entire design, i.e., both pads and lines, resulted in a highly uniform pattern, as seen in the inset in Fig. 7(a). To avoid damage of the smaller pads in the interconnect patterns by the probes used for electrical characterization, additional sets of patterns were printed with the smaller pads overlapping with larger e-beam deposited Au pads on glass substrates, as shown in the optical micrograph in Fig. 7(c). The LDT printed lines displayed Ohmic resistive behavior, as shown by the inset plot, with values between  $0.7$  and  $0.9 \Omega$  corresponding to a resistivity of  $\sim 6.5 \mu\Omega \text{ cm}$  (roughly  $4\times$  bulk Ag). In this exercise, each entire interconnect was LDT printed with one single laser pulse rather than generating it by fusing many individual smaller voxels. The use of a DMD to shape the LDT-generated voxel allowed the interconnect design to be quickly updated between laser pulses ( $<1 \text{ ms}$  for up to  $1 \text{ kHz}$  laser firing rates), demonstrating the concept of printing dynamically reconfigurable voxels.

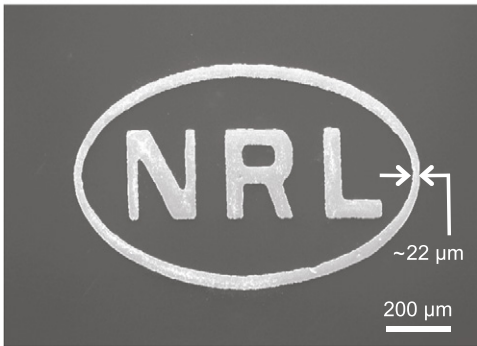
Laser-printed patterns using high-viscosity NP pastes offer many advantages over those made from lower-viscosity NP inks. The transferred voxels are congruent with the shape and size of the incident laser beam profile, thereby allowing arbitrary digitization of the printed voxels, especially when printed with laser pulses shaped by a spatial light modulator.



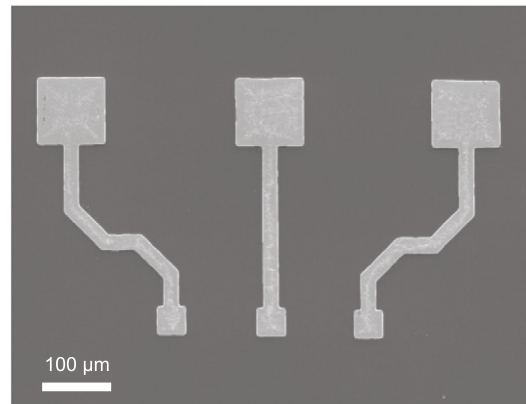
(a)



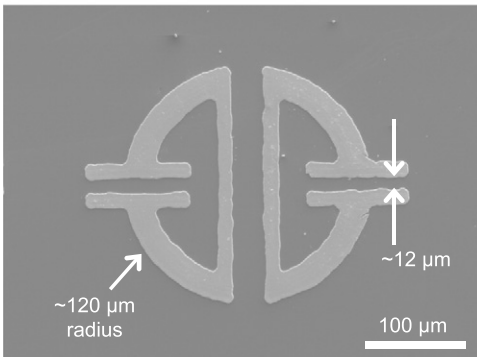
(a)



(b)



(b)

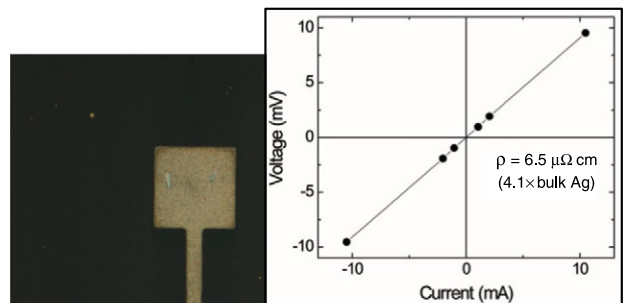


(c)

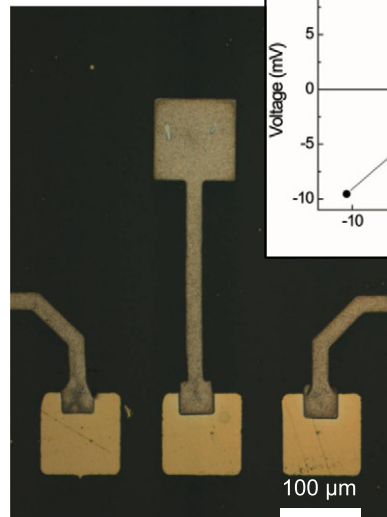
**Figure 6.** Examples of entire structures printed with a single laser pulse by LDT of high-viscosity Ag NP pastes to generate (a) a freestanding microbridge (no sacrificial layers were used), (b) an arbitrary pattern over a large area (the NRL logo is over 1 mm long) and (c) a metamaterial inspired D-ring antenna.

The high-viscosity NP paste eliminates many of the wetting issues between the substrate surface and the deposited material, a problem commonly encountered in printing processes using low-viscosity inks. Minimizing these substrate wetting effects means that higher tolerances can be held between the desired design and the generated pattern. The use of a DMD to shape the laser beam profile provides an additional capability by allowing the voxel to be adjusted dynamically, effectively parallelizing the printing process.

Despite these advantages, large area printing of high-viscosity NP pastes is limited by the ability to apply the NP paste to the ribbon over large areas ( $>1 \text{ cm}^2$ ) while maintaining its thickness uniformity to within 100s of nm.



(c)



(c)

**Figure 7.** (a)–(b) SEM images of 2D interconnect patterns generated with the DMD and printed by LDT. (a) Straight interconnect with the inset showing higher magnification detail of a larger pad ( $L = 250 \mu\text{m}$  and  $W = 25 \mu\text{m}$ ). (b) Set of three interconnect patterns, each one printed with one single laser pulse by LDT of high-viscosity Ag NP paste. (c) Optical micrograph of a set of interconnects printed over Au pads on a glass substrate. The inset shows the  $I$ – $V$  plot of one of these interconnects, confirming its ohmic behavior with  $6.5 \mu\Omega \text{ cm}$  resistivity.

If the laser energy is too low (or the thickness of the layer too high) the voxel will not be released from the ribbon,

while if the energy is too high (or the thickness too low) the voxel will be released with excess energy, leading to its spreading, splashing or even fracturing as it lands on the receiving substrate. In both cases, thickness uniformity of the NP ink or paste and a constant gap between the ink layer and the receiving substrate over the area being patterned must be maintained in order to guarantee the transfer of intact voxels at the optimized laser pulse energies. Lower-viscosity inks are easily spin-coated into a uniform layer on the ribbon while high-viscosity NP pastes cannot be applied in this manner. Overcoming these implementation challenges is the focus of our current research efforts, with the goal of facilitating the transition of LIFT and LDT from research tools to the microelectronics-manufacturing arena.

## CONCLUSIONS

The use of laser forward transfer techniques for the printing of silver NP suspensions offers significant opportunities for the direct-write of electrically conductive patterns for microelectronic applications requiring the digital fabrication of interconnects, electrodes, antennas and passive devices. The use of low-viscosity silver NP inks with LIFT results in the transfer of drop-shaped voxels that are subject to wetting effects upon contact with the receiving substrates. By adjusting the spacing between discrete voxels, continuous lines are generated as they coalesce. However, the resolution of the printed pattern is a function of the ink-substrate interaction, in a manner similar to inkjet printing. A better approach is to take advantage of the nozzle-free capability of laser transfer to print high-viscosity NP pastes by LDT. Under the right conditions, LDT allows for minimal deformation of the voxel as it is released from the ribbon and lands on the receiving substrate. As such, LDT is unique in its ability to generate voxels congruent with the laser pulse over a large range of sizes (from microns to millimeters). Finally, by spatially adjusting the laser pulse used with LDT, with a micromirror-based spatial light modulator, it is possible to print dynamically reconfigurable voxels. That is, each voxel can vary in size and shape from the previous one, thus allowing faster pattern generation and overall optimization of the sequence of printing steps required to generate a full design. The combination of LDT with DMDs is a potentially disruptive technology in the field of digital fabrication since it can be used to transform what was considered until now to be a serial process into a parallel printing technique.

## ACKNOWLEDGMENT

This work was funded by the Office of Naval Research (ONR) through the Naval Research Laboratory Basic Research Program.

## REFERENCES

- <sup>1</sup> A. Piqué and D. B. Chrisey, *Direct-Write Technologies for Rapid Prototyping Applications* (Academic Press, San Diego, 2002).
- <sup>2</sup> K. K. B. Hon, L. Li, and I. M. Hutchings, "Direct writing technology-Advances and developments," *CIRP Annals - Manufacturing Technol.* **57**, 601–620 (2008).
- <sup>3</sup> Y. Zhang, C. Liu, and D. Whalley, "Direct-write techniques for maskless production of microelectronics: a review of current state-of-the-art technologies," *Int'l. Conf. on Electronic Packaging Technol. and High Density Packaging*, ICEPT-HDP 2009, art. no. 5270702, pp. 497–503 (2009).
- <sup>4</sup> P. Calvert, "Inkjet printing for materials and devices," *Chem. Mater.* **13**, 3299–3305 (2001).
- <sup>5</sup> J. Stringer and B. Derby, "Limits to feature size and resolution in ink jet printing," *J. Eur. Ceramic Soc.* **29**, 913–918 (2009).
- <sup>6</sup> H. Kang, D. Soltman, and V. Subramanian, "Hydrostatic optimization of inkjet-printed films," *Langmuir* **26**, 11568–11573 (2010).
- <sup>7</sup> C. B. Arnold, P. Serra, and A. Piqué, "Laser direct-write techniques for printing of complex materials," *MRS Bulletin* **32**, 23–31 (2007).
- <sup>8</sup> M. Duocastella, H. Kim, P. Serra, and A. Piqué, "Optimization of laser printing of nanoparticle suspensions for microelectronic applications," *Appl. Phys. A: Mater. Sci. Process.* **106**, 471–478 (2012).
- <sup>9</sup> A. Piqué, R. C. Y. Auyeung, H. Kim, K. M. Metkus, and S. A. Mathews, "Digital microfabrication by laser decal transfer," *J. Laser Micro/Nanoeng* **3**, 163 (2008).
- <sup>10</sup> A. Piqué, R. C. Y. Auyeung, K. Metkus, H. Kim, S. A. Mathews, T. Bailey, X. Chen, and L. J. Young, "Laser decal transfer of electronic materials with thin film characteristics," *Proc. SPIE* **6879**, 687911 (2008).
- <sup>11</sup> H. Kim, J. S. Melinger, A. Khachatryan, N. A. Charipar, R. C. Y. Auyeung, and A. Piqué, "Fabrication of terahertz metamaterials by laser printing," *Opt. Lett.* **35**, 4039–4041 (2010).
- <sup>12</sup> J. Wang, R. C. Y. Auyeung, H. Kim, N. A. Charipar, and A. Piqué, "Three-dimensional printing of interconnects by laser direct-write of silver nanopastes," *Adv. Mater.* **22**, 4462–4466 (2010).
- <sup>13</sup> R. C. Y. Auyeung, H. Kim, A. J. Birnbaum, M. Zalalutdinov, S. A. Mathews, and A. Piqué, "Laser decal transfer of freestanding microcantilevers and microbridges," *Appl. Phys. A: Mater. Sci. Process.* **97**, 513–519 (2009).
- <sup>14</sup> A. J. Birnbaum, R. C. Y. Auyeung, K. J. Wahl, M. Zalalutdinov, A. R. Laracuate, and A. Piqué, "Laser printed micron-scale free standing laminate composites: process and properties," *J. Appl. Phys.* **108**, 083526 (2010).
- <sup>15</sup> A. J. Birnbaum, M. K. Zalalutdinov, K. J. Wahl, and A. Piqué, "Fabrication and response of laser printed cavity sealing membranes," *J. Microelectromech. Syst.* **20**, 436–440 (2011).
- <sup>16</sup> D. Soltman, B. Smith, H. Kang, S. J. S. Morris, and V. Subramanian, "Methodology for inkjet printing of partially wetting films," *Langmuir* **26**, 15686–15693 (2010).
- <sup>17</sup> R. C. Y. Auyeung, H. Kim, N. Charipar, A. Birnbaum, S. Mathews, and A. Piqué, "Laser forward transfer based on a spatial light modulator," *Appl. Phys. A: Mater. Sci. Process.* **102**, 21–26 (2011).
- <sup>18</sup> A. Piqué, R. C. Y. Auyeung, A. T. Smith, H. Kim, S. A. Mathews, N. A. Charipar, and M. A. Kirleis, "Laser transfer of reconfigurable patterns with a spatial light modulator," *Proc. SPIE* **8608**, 86080K (2013).
- <sup>19</sup> H. Kim, R. C. Y. Auyeung, S. H. Lee, A. L. Huston, and A. Piqué, "Laser-printed interdigitated Ag electrodes for organic thin film transistors," *J. Phys. D: Appl. Phys.* **43**, 085101 (2010).
- <sup>20</sup> R. C. Y. Auyeung, H. Kim, S. A. Mathews, and A. Piqué, "Laser direct-write of metallic nanoparticle inks," *J. Laser Micro/Nanoeng.* **2**, 21–25 (2007).
- <sup>21</sup> M. Baum, H. Kim, I. Alexeev, A. Piqué, and M. Schmidt, "Generation of transparent conductive electrodes by laser consolidation of LIFT printed ITO nanoparticle layers," *Appl. Phys. A: Mater. Sci. Process.* **111**, 799–805 (2013).
- <sup>22</sup> H. Kim, G. P. Kushto, C. B. Arnold, Z. H. Kafafi, and A. Piqué, "Laser processing of nanocrystalline TiO<sub>2</sub> films for dye-sensitized solar cells," *Appl. Phys. Lett.* **85**, 464–466 (2004).
- <sup>23</sup> J. Lewis, "Direct ink writing of 3D functional materials," *Adv. Funct. Mat.* **16**, 2193–2204 (2006).
- <sup>24</sup> A. Palla-Papavlu, C. Córdoba, A. Patrascioiu, J. M. Fernández-Pradas, J. L. Morenza, and P. Serra, "Deposition and characterization of lines printed through laser-induced forward transfer," *Appl. Phys. A: Mater. Sci. Process.* **110**, 751–755 (2013).
- <sup>25</sup> B. J. Kang and J. H. Oh, "Geometrical characterization of inkjet-printed conductive lines of nanosilver suspensions on a polymer substrate," *Thin Solid Films* **518**, 2890–2896 (2010).
- <sup>26</sup> A. J. Birnbaum, H. Kim, N. A. Charipar, and A. Piqué, "Laser printing of multi-layered polymer/metal heterostructures for electronic and MEMS devices," *Appl. Phys. A: Mater. Sci. Process.* **99**, 711–716 (2010).